Check for updates

Received: 3 July 2023 | Revised: 15 May 2024 | Accepted: 15 June 2024

DOI: 10.1002/nbm.5212

RESEARCH ARTICLE

NMR IN BIOMEDICINE WILEY

Probing diffusion of water and metabolites to assess white matter microstructure in Duchenne muscular dystrophy

Rosanne Govaarts[1,5] | Nathalie Doorenweerd[1,2] | Chloé F. Najac[1] | Emma M. Broek[1] | Maud E. Tamsma[1] | Kieren G. Hollingsworth[3] | Erik H. Niks[4,5] | Itamar Ronen[1,6] | Volker Straub[2] | Hermien E. Kan[1,5]

[1]C.J. Gorter MRI Center, Department of Radiology, Leiden University Medical Center, Leiden, The Netherlands

[2]John Walton Muscular Dystrophy Research Centre, Newcastle University and Newcastle Hospitals NHS Foundation Trust, Newcastle upon Tyne, UK

[3]Translational and Clinical Research Institute, Faculty of Medical Sciences, Newcastle University, Newcastle upon Tyne, UK

[4]Department of Neurology, Leiden University Medical Center, Leiden, The Netherlands

[5]Duchenne Centre Netherlands, Leiden, The Netherlands

[6]Clinical Imaging Sciences Centre, Brighton and Sussex Medical School, Brighton, UK

Correspondence
Rosanne Govaarts, Department of Radiology, Leiden University Medical Center, C-03-Q, P.O. Box 9600, 2300 RC Leiden, The Netherlands.
Email: r.a.a.m.govaarts@lumc.nl

Funding information
This study was funded by Duchenne Parent Project Netherlands (Brain imaging and cognition in Duchenne muscular dystrophy—2010), Muscular Dystrophy UK (grant RA3/2079/1), and Gratama Foundation Netherlands (Leiden University, grant 10.13). RG receives funding from the European Union's Horizon 2020 research and innovation programme under grant agreement 847826.

Duchenne muscular dystrophy (DMD) is a progressive X-linked neuromuscular disorder caused by the absence of functional dystrophin protein. In addition to muscle, dystrophin is expressed in the brain in both neurons and glial cells. Previous studies have shown altered white matter microstructure in patients with DMD using diffusion tensor imaging (DTI). However, DTI measures the diffusion properties of water, a ubiquitous molecule, making it difficult to unravel the underlying pathology. Diffusion-weighted spectroscopy (DWS) is a complementary technique which measures diffusion properties of cell-specific intracellular metabolites. Here we performed both DWS and DTI measurements to disentangle intra- and extracellular contributions to white matter changes in patients with DMD. Scans were conducted in patients with DMD (15.5 ± 4.6 y/o) and age- and sex-matched healthy controls (16.3 ± 3.3 y/o). DWS measurements were obtained in a volume of interest (VOI) positioned in the left parietal white matter. Apparent diffusion coefficients (ADCs) were calculated for total *N*-acetylaspartate (tNAA), choline compounds (tCho), and total creatine (tCr). The tNAA/tCr and tCho/tCr ratios were calculated from the non-diffusion-weighted spectrum. Mean diffusivity (MD), radial diffusivity (RD), axial diffusivity (AD), and fractional anisotropy of water within the VOI were extracted from DTI measurements. DWS and DTI data from patients with DMD (respectively $n = 20$ and $n = 18$) and $n = 10$ healthy controls were included. No differences in metabolite ADC or in concentration ratios were found between patients with DMD and controls. In contrast, water diffusion (MD, $t = -2.727$, $p = 0.011$; RD, $t = -2.720$, $p = 0.011$; AD, $t = -2.715$, $p = 0.012$) within the VOI was significantly higher in patients compared with healthy controls. Taken together, our study illustrates the potential of combining DTI and DWS to gain a better understanding of microstructural changes and their association with disease mechanisms in a clinical setting.

Abbreviations: AD, axial diffusivity; ADC, apparent diffusion coefficient; AQP4, acquaporin-4 water channel; BET, Brain Extraction Tool; CRLB, Cramér–Rao lower bound; DMD, Duchenne muscular dystrophy; DTI, diffusion tensor imaging; DWS, diffusion-weighted spectroscopy; FA, fractional anisotropy; FAST, FMRIB's automated segmentation tool; FSL, FMRIB Software Library; FWHM, full-width at half-maximum; GLM, general linear model; GPC, glycerophosphocholine; HC, healthy control; MD, mean diffusivity; NAA, *N*-acetylaspartate; NAAG, *N*-acetyl-aspartyl-glutamate; n/a, not applicable; RD, radial diffusivity; PRESS, point resolved spectroscopy; SNR, signal-to-noise ratio; tCho, choline compounds; tCr, total creatine; TE, echo time; tNAA, total NAA; TR, repetition time; VOI, volume of interest.

This is an open access article under the terms of the Creative Commons Attribution License, which permits use, distribution and reproduction in any medium, provided the original work is properly cited.
© 2024 The Author(s). *NMR in Biomedicine* published by John Wiley & Sons Ltd.

KEYWORDS
brain, diffusion tensor imaging, diffusion-weighted spectroscopy, Duchenne muscular dystrophy, MRI, multimodal, white matter

1 | INTRODUCTION

Duchenne muscular dystrophy (DMD) is a hereditary recessive X-linked neuromuscular disorder caused by mutations in the dystrophin-encoding *DMD* gene. Dystrophin is expressed in numerous tissues in the body, including muscle and brain. DMD is characterized by progressive muscle weakness. Common early symptoms of DMD include difficulty standing and walking, followed by wheelchair dependence around 12 years of age. Eventually, DMD will lead to a premature death around the age of 30 due to respiratory failure or cardiomyopathy. In addition to muscular symptoms, a subset of patients with DMD present with cognitive, emotional, learning, and behavioural complaints.[1–8]

The *DMD* gene encodes for multiple dystrophin isoforms, of which Dp427, Dp140, Dp71, and Dp40 are expressed in the brain.[9–16] As DMD is caused by mutations within the *DMD* gene, the site of the mutation can result in the absence of one or more dystrophin isoforms. Approximately 50% of patients with DMD have a mutation only affecting Dp427, and 48% also lack Dp140. Patients missing all isoforms represent 1%–2% of the population. The different isoforms in DMD are associated with different cell types: Dp427 with neurons and Dp140 and/or Dp71 with astrocytes.[17,18] Roles of these isoforms in early development and axonal guidance (Dp140) or in cerebral vasculature and pericytes (Dp71) have been proposed. However, the effect of dystrophin absence on these processes has not yet been investigated.[19–21] In addition, there is further evidence for an important role for astrocytes with the study of induced pluripotent stem cells from patients with DMD,[21] where all DMD astrocytes tested displayed altered morphology, altered proliferative activity, and decreased aquaporin-4 water channel (AQP4) expression. Due to the different cellular expressions of these isoforms, the neuronal compartment is hypothesized to be affected in all DMD patients, and the glial compartment to be additionally affected in half of the patients.

Previous MRI studies showed an overall decreased grey matter volume on T_1-weighted images and reduced cerebral blood flow on perfusion images in the DMD brain.[22,23] Bioenergetic changes, such as an increase in inorganic phosphate to adenosine triphosphate ratio, were previously reported in young DMD boys using ^{31}P MRS.24 Studies using ^{1}H MRS focused on changes in *N*-acetylaspartate (NAA) and choline compounds (tCho), markers of neurons and glial metabolism, respectively.[25–27] While one study showed a significant increase in the ratio of tCho/NAA in the left cerebellum and no changes in the left frontal lobe of DMD patients,[28] another study showed no changes in various brain regions, including cerebellum.[29] Diffusion tensor imaging (DTI) studies showed decreased fractional anisotropy (FA) and increased mean diffusivity (MD), indicating altered white matter microstructure.[30,31] However, the underlying process by which the absence of dystrophin results in altered microstructure remains unclear. DTI only probes the diffusion of water, which is a ubiquitous marker that is present in all compartments.[25] By contrast, diffusion-weighted spectroscopy (DWS) can probe the diffusion properties of brain metabolites, which are compartment- and cell-specific endogenous markers.[25–27] To the best of our knowledge, no previous studies have investigated changes in brain metabolite diffusion in the brain of DMD patients.

This study investigated the intra- versus extracellular contribution to white matter differences seen in patients with DMD. To this end, DWS and DTI measurements were combined within the same volume of interest (VOI).

2 | METHODS

2.1 | Participants

Two cross-sectional studies were performed in collaboration between Leiden University Medical Center (Leiden, The Netherlands) and Newcastle University (Newcastle upon Tyne, UK). The studies were approved by the local medical ethical committees. Written informed consent was obtained from all participants and/or their legal guardians prior to the study. Patients with DMD were recruited from patient registries, local clinics, and flyers. Inclusion criteria were a genetically confirmed DMD diagnosis, being over 8 years old, and having the ability to lie supine for at least 30 min. As a classification of muscle function to indicate the stage of the disease, the Brooke scale for upper extremity function and Vignos scale for lower extremity function were assessed.[32] Wheelchair bound was defined as not being able to walk for 10 m without support. Healthy controls were recruited through flyers at local schools and sports clubs. MRI contraindications were exclusion criteria for all.

No stratification was performed for corticosteroid schedules or other medication use. Patients were not selected for mutation type or cognitive problems to acquire a random sample of the genetic and neurocognitive phenotypes. Dystrophin isoform expression was derived for all patients with DMD from the pre-established mutation in the *DMD* gene. A proximal mutation was defined as upstream of intron 44, affecting the full-length dystrophin isoform Dp427. A distal mutation was defined as downstream of exon 50, affecting Dp427, Dp140, and in some cases even Dp71.[33]

10991492, 0, Downloaded from https://analyticalsciencejournals.onlinelibrary.wiley.com/doi/10.1002/nbm.5212 by Newcastle University, Wiley Online Library on [24/07/2024]. See the Terms and Conditions (https://onlinelibrary.wiley.com/terms-and-conditions) on Wiley Online Library for rules of use; OA articles are governed by the applicable Creative Commons License

2.2 | MR data acquisition

At both study sites, scans were obtained using a 3 T MRI scanner (Philips Achieva, Best, The Netherlands), using an eight-channel head coil, identical scanning protocol, and software versions 3.2.3 and 5.1.7 for the NL and UK, respectively.

3D T_1-weighted scans (echo time/repetition time (TE/TR) 4.6/9.8 ms; spatial resolution 1.17 × 0.92 × 1.17 mm; 4 min 55 s) were obtained for anatomical reference and used for planning the VOI for DWS. A 30 × 20 × 15 mm^3 VOI was positioned in the parietal left white matter (see Figure 1). The position of the VOI was based on previous DTI results showing increased MD in this area,[23] as well as the practical consideration of consistently obtaining predominantly white matter content of a large VOI. DWS data were acquired with (24 signal averages) and without (2 signal averages) water suppression and using a cardiac-triggered diffusion-weighted PRESS sequence ($TE = 125$ ms, $TR = 2$ cardiac cycles; $\Delta/\delta = 73/27$ ms; $b = 0$ and $b = 3765$ mm^2/s; three orthogonal diffusion directions; total acquisition time 3 min 44 s, Table S1).[25] DTI scans (TE/TR 59/9440 ms; spatial resolution 1.96 × 2 × 2 mm^3; 32 directions, $b = 0$ and $b = 1000$ s/mm^2; 6 min 40 s) were obtained to determine water diffusion properties.

2.3 | Data processing

2.3.1 | Anatomical images (T_1)

T_1-weighted images were segmented into probabilistic tissue maps for cerebrospinal fluid (CSF), grey matter, and white matter using the the FMRIB Software Library (FSL) Brain Extraction Tool (BET)[34] and the FMRIB's automated segmentation tool (FAST).[35, 36] A custom-made MATLAB routine (MathWorks, Natick, MA, USA) was then used to align the DWS VOI on the tissue map, and used to extract the volume fraction of each tissue type within the VOI.

2.3.2 | Metabolite diffusion (DWS)

Spectral processing

Processing of the DWS data was conducted with a custom-made MATLAB routine. Spectra were corrected for zero-order phasing, individual phase and frequency drift based on residual water, and eddy currents based on non-water-suppressed data. Individual spectra were

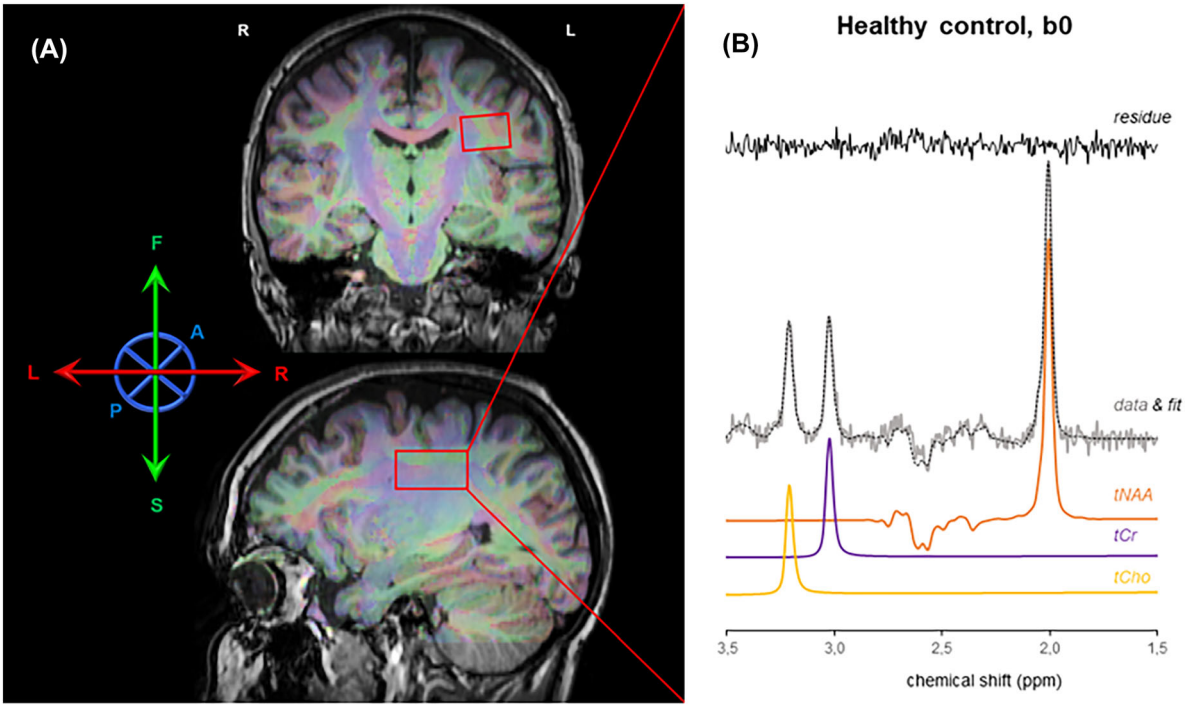

FIGURE 1 Placement of the VOI overlaid on the FA map and an example of a fitted non-diffusion-weighted spectrum. A, Illustration of an overlaid T_1 image, a DTI colour-coded FA map, and the placement of the VOI (red box) of the DWS scan. B, Example of a fitted non-DW spectrum in LCModel for an HC. Shown are three individual metabolite fits, for tNAA, tCr, and tCho.

10991492, 0, Downloaded from https://analyticalsciencejournals.onlinelibrary.wiley.com/doi/10.1002/nbm.5212 by Newcastle University, Wiley Online Library on [24/07/2024]. See the Terms and Conditions (https://onlinelibrary.wiley.com/terms-and-conditions) on Wiley Online Library for rules of use; OA articles are governed by the applicable Creative Commons License

retrospectively rejected to filter out outliers due to poor cardiac triggers. Spectra were averaged, resulting in four spectra (one $b = 0$ and three directions with $b = 3765$ mm^2/s).

Spectra were analysed with LCModel[37] and using a MATLAB-generated basis set using the density matrix formalism.[38] The basis set was simulated for the point resolved spectroscopy (PRESS) sequence with $T_E = 125$ ms, identical to our acquisition. Simulations were performed using infinitely short hard pulse, namely ideal or impulse RF pulse, meaning that we assumed no time evolution during the pulses. We used known chemical shifts and *J*-coupling constants of the proton resonances of the metabolites.[38] The basis set included a total of 19 metabolites: alanine, aspartate, choline, creatine, GABA, glucose, glutamine, glutamate, glycerophosphocholine (GPC), glutathione, myo-inositol, lactate, phosphocreatine, phosphocholine, phosphoethanolamine, NAA, *N*-acetylaspartylglutamate, taurine, and scyllo-inositol.[25] We did not include any macromolecules due to our long T_E. Spectral quality was deemed sufficient if signal-to-noise ratio (SNR) was greater than 6, full-width at half-maximum (FWHM) for NAA was less than 3.83 Hz, and Cramér–Rao lower bounds (CRLBs) were less than 6% for NAA and less than 10% for choline and creatine. We could reliably measure the signal of total NAA (tNAA = NAA + *N*-acetyl-aspartyl-glutamate (NAAG)), tCho (tCho = choline + phosphocholine + GPC), and total creatine (tCr = creatine + phosphocreatine).

Quantification of metabolite diffusion

Metabolite apparent diffusion coefficients (ADCs) were calculated for the three orthogonal diffusion directions. Assuming a mono-exponential decay over our *b* values the following formula[25] is applied:

$$\mathrm{ADC}_i = -\frac{\ln\left(\frac{S(b)_i}{S(0)}\right)}{b},$$

where $S(b)_i$ is the measured signal with the DW gradient applied in direction *i*, and $S_{(0)}$ is the signal without diffusion weighting. The ADC_i coefficients of all three directions *i* were finally averaged to obtain the ADC of tNAA, tCho, and tCr. We opted to normalize our metabolite signals, measured using non-diffusion-weighted spectra, to an internal reference, namely tCr.[39] This is based on the assumption that there are no changes in tCr between healthy controls and DMD patients.

Water diffusion (DTI)

DTI data were pre-processed using ExploreDTI[40] and included signal drift, Gibbs ringing, subject motion, eddy current, and echo planar imaging corrections. DTI data were registered to the 3D T_1-weighted image using SPM8. Subsequently, maps of the relevant diffusion metrics (MD, radial diffusivity (RD), axial diffusivity (AD), and FA) were extracted for each subject using ExploreDTI.[40] Using a custom-made MATLAB routine diffusion metrics within the VOI were extracted.

2.4 | Statistics

The two study sites and between-group differences determined for tissue volume fraction and age were tested to assess the need to include these as covariates using *t*-tests. Tissue volume fraction and age did not differ between study sites or between DMD and healthy controls (HCs) ($p > 0.05$), and were therefore not included as covariate in further analyses. To account for inter-dependences between metabolites, a multivariate general linear model (GLM) was used to assess the difference in ADCs of tNAA, tCho, and tCr between patients with DMD and HC.

Independent two-tailed sample *t*-tests were used to assess differences between patients with DMD and HCs in the ratios of tNAA:tCr and tCho:tCr, as well as MD from DTI. Post hoc testing was performed with independent sample *t*-tests to assess group differences in RD, AD, and FA. Results of *t*-tests and GLM were considered significant at $p < 0.05$. All statistical tests were carried out using IBM SPSS Version 25.0.

3 | RESULTS

3.1 | Participant characteristics and data inclusion

In this study $n = 28$ genetically confirmed patients with DMD and $n = 17$ age- and sex-matched HCs were recruited. From this cohort, DWS data were available for $n = 23$ patients with DMD and $n = 13$ HCs. Data from $n = 20$ patients with DMD (age 15.5 ± 4.6 years) and $n = 10$ HC (age 16.3 ± 3.3 years) passed quality control and were included in further analyses. For DTI, scans from another two participants showed severely warped scans that could not be corrected, and therefore were excluded from DTI analyses. See Table 1 for participant characteristics of the included patients and Figure 2 for the data inclusions in the study. Tissue volume fraction and age did not differ between study sites or between DMD and HC ($p > 0.05$). The VOI placement for all subjects can be found in Figure S1.

10991492, 0, Downloaded from https://analyticalsciencejournals.onlinelibrary.wiley.com/doi/10.1002/nbm.5212 by Newcastle University, Wiley Online Library on [24/07/2024]. See the Terms and Conditions (https://onlinelibrary.wiley.com/terms-and-conditions) on Wiley Online Library for rules of use; OA articles are governed by the applicable Creative Commons License

TABLE 1 Participant characteristics.

	DMD			Control		
	Total	NL	UK	Total	NL	UK
General characteristics						
N	20	9	11	10	6	4
Age (years)[a]	15.5 ± 4.6	15.7 ± 4.5	15.4 ± 5.0	16.3 ± 3.3	16.2 ± 2.6	16.5 ± 4.6
Age (range)	10.6–23.8	10.6–22.8	10.9–23.8	11.8–22.3	11.9–18.9	11.8–22.3
Steroid treatment	19	9	10	n/a	n/a	n/a
Prednisolone (intermittent)	10	8	2	n/a	n/a	n/a
Prednisolone (daily)	3	0	3	n/a	n/a	n/a
Deflazacort (daily)	4	1	3	n/a	n/a	n/a
Unknown	0	0	2	n/a	n/a	n/a
White matter fraction (%)[a]	77.7 ± 9.5	77.9 ± 10.7	77.6 ± 8.9	80.1 ± 9.7	77.4 ± 10.7	84.3 ± 7.4
Wheelchair bound	10	3	7	n/a	n/a	n/a
Brooke score[a]	2.0 ± 1.4	1.4 ± 1.0	2.5 ± 1.6	1.0 ± 0	1.0 ± 0	1.0 ± 0
Vignos score[a]	4.8 ± 3.1	3.6 ± 2.3	5.7 ± 3.4	1.0 ± 0	1.0 ± 0	1.0 ± 0
Dystrophin mutation						
Proximal, *n* =	11	6	5	n/a	n/a	n/a
Distal, *n* =	6	2	4	n/a	n/a	n/a
Unclassified, *n* =	3	1	2	n/a	n/a	n/a

Abbreviations: DMD, Duchenne muscular dystrophy; N or n, number; n/a, not applicable; NL, Netherlands; UK, United Kingdom.
[a]Data are presented as mean ± SD.

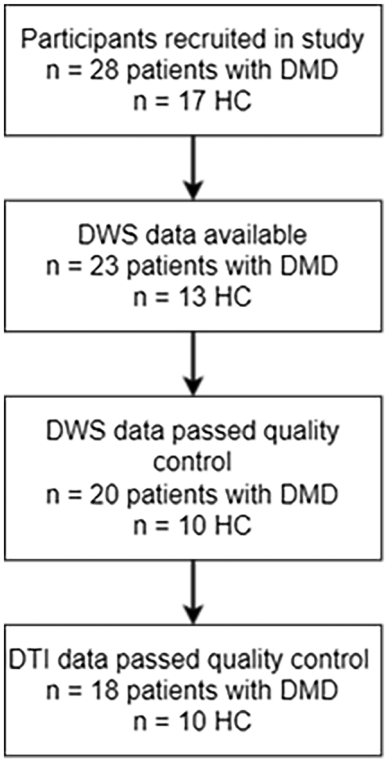

FIGURE 2 Data inclusions for analyses.

10991492, 0, Downloaded from https://analyticalsciencejournals.onlinelibrary.wiley.com/doi/10.1002/nbm.5212 by Newcastle University, Wiley Online Library on [24/07/2024]. See the Terms and Conditions (https://onlinelibrary.wiley.com/terms-and-conditions) on Wiley Online Library for rules of use; OA articles are governed by the applicable Creative Commons License

3.2 | Metabolite diffusion (DWS)

Representative DWS spectra at $b = 0$ and $b = 3765$ mm^2/s are shown in Figure 3. The SNR of the DWS spectra was 18.6 ± 4.1 for the b_0 spectra and 8.4 ± 2.3 for the b_{3765} spectra. The FWHM of the NAA peak was 3.58 ± 0.89 and 3.96 ± 1.15 Hz for b_0 and b_{3765} spectra, respectively. The

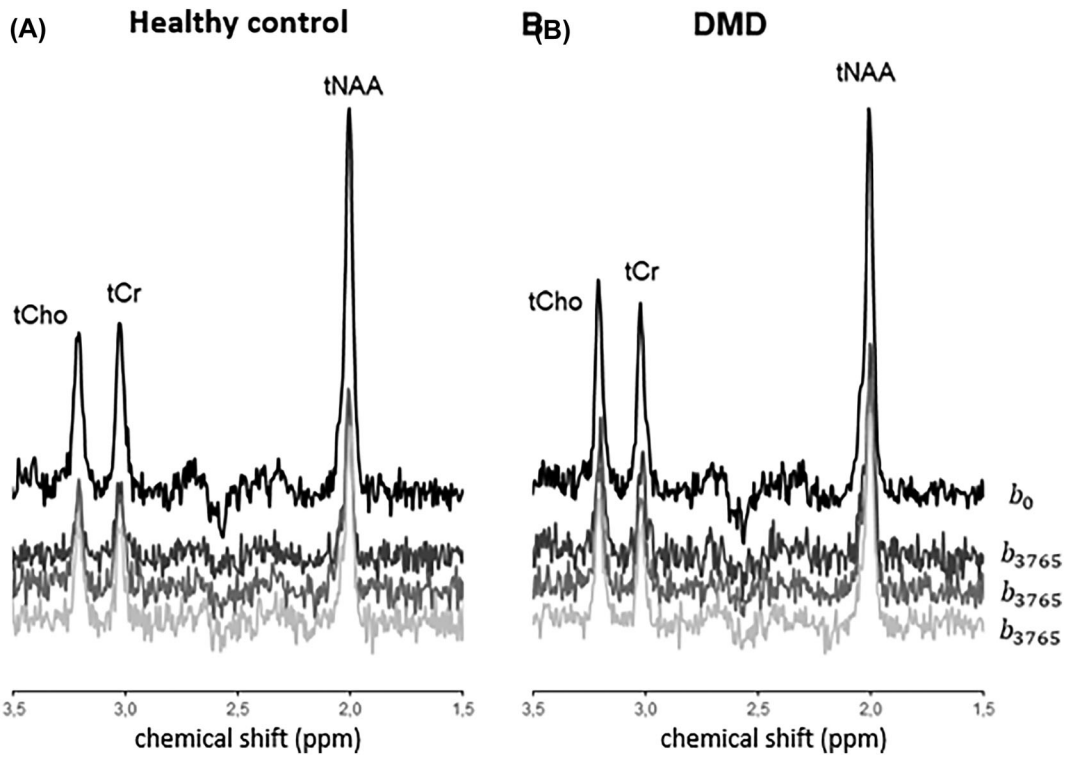

FIGURE 3 Representative examples of an averaged spectrum for an HC (A) and a DMD patient (B), showing tCho, tCr, and tNAA peaks. The average non-diffusion-weighted spectrum (in black) and the average diffusion-weighted spectra in three directions (in grey) are depicted.

TABLE 2 DWS metabolite ADCs and ratios and DTI diffusivity metrics for patients with DMD and HCs.

	DMD		HC		
	n	Mean ± SD	*n*	Mean ± SD	Significance
ADC					
tNAA (μm^2/ms)	20	0.165 ± 0.019	10	0.168 ± 0.020	$F(1, 29) = 0.221$, $p = 0.642$
tCr (μm^2/ms)	20	0.170 ± 0.022	10	0.169 ± 0.023	$F(1, 29) = 0.008$, $p = 0.928$
tCho (μm^2/ms)	20	0.157 ± 0.037	10	0.138 ± 0.023	$F(1, 29) = 2.099$, $p = 0.129$
Metabolite ratios					
tNAA:tCr	20	2.45 ± 0.21	10	2.41 ± 0.15	$t = -0.587$, $p = 0.562$
tCho:tCr	20	0.35 ± 0.06	10	0.32 ± 0.03	$t = -1.534$, $p = 0.136$
DTI metrics					
MD (μm^2/ms)	18	1.049 ± 0.083	10	0.972 ± 0.041	$t = -2.727$, $p = 0.011$*
RD (μm^2/ms)	18	0.941 ± 0.080	10	0.866 ± 0.042	$t = -2.720$, $p = 0.011$*
AD (μm^2/ms)	18	1.266 ± 0.089	10	1.1184 ± 0.042	$t = -2.715$, $p = 0.012$*
FA	18	0.215 ± 0.009	10	0.221 ± 0.013	$t = 1.128$, $p = 0.212$

Abbreviations: DMD, Duchenne muscular dystrophy; n, number; SD, standard deviation; ADC, apparent diffusion coefficients; tNAA, total N-acetyl aspartate; tCR, total creatine, tCho, choline compounds, DTI, diffusion tensor imaging; MD, mean diffusivity; RD, radial diffusivity; AD, axial diffusivity, FA, fractional anisotropy .
Note: Data are expressed as mean ± SD. Test and *p*-values are reported in the last column.
*Significance level was set at $p < 0.05$.

10991492, 0, Downloaded from https://analyticalsciencejournals.onlinelibrary.wiley.com/doi/10.1002/nbm.5212 by Newcastle University, Wiley Online Library on [24/07/2024]. See the Terms and Conditions (https://onlinelibrary.wiley.com/terms-and-conditions) on Wiley Online Library for rules of use; OA articles are governed by the applicable Creative Commons License

CRLBs (%) for NAA were 1.8 ± 0.5 for condition b_0 and 3.6 ± 0.8 for condition b_{3765}, indicating low uncertainty of the metabolite level estimated using LCModel. For tCho and tCr, CRLBs (%) were 4.2 ± 0.7 and 3.5 ± 0.7 in the b_0 condition, increasing to 8.3 ± 2.2 and 6.8 ± 1.9 in the b_{3765} conditions respectively. This is well within the quality limit of CRLBs defined at the start of the study.

None of the metabolite ADCs differed between the groups (Table 2 and Figure 4). The metabolite ratios of tNAA/tCr and tCho/tCr for HC and patients with DMD also did not differ between groups (Figure 5 and Table 2).

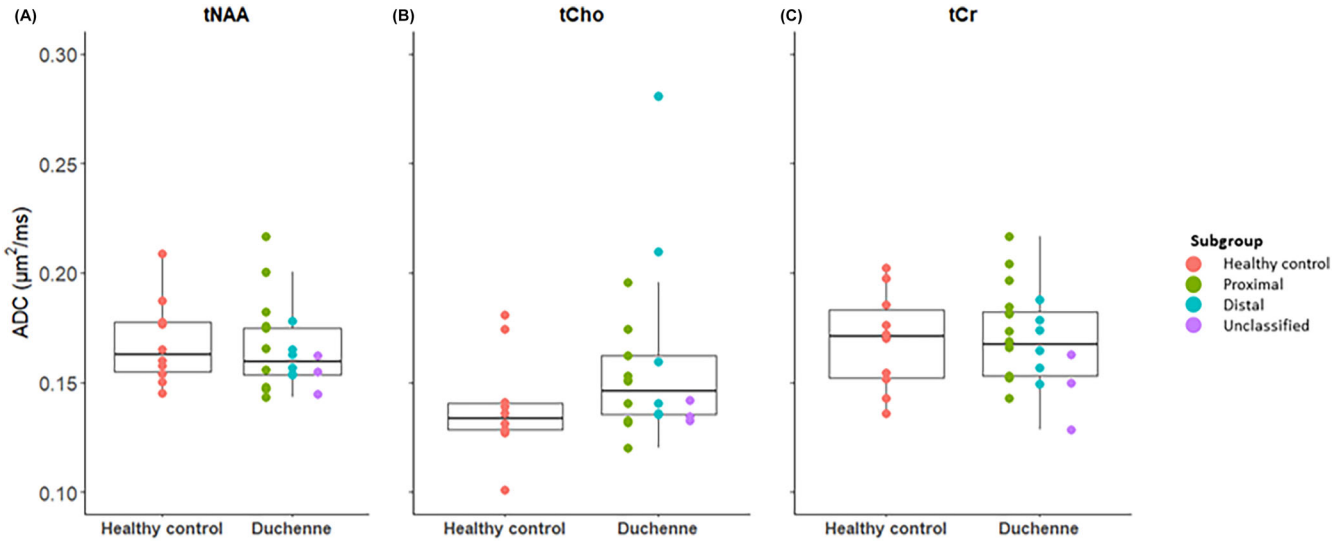

FIGURE 4 Scatterplots for the ADCs of tNAA (A), tCho (B), and tCr (C). For the Duchenne subgroup, a proximal mutation affects the Dp427 form only (i.e., assumed to be linked to neurons) and distal corresponds to a mutation affecting both Dp427 and Dp140 forms (i.e., assumed to be linked to neurons and glial cells). None of the between-group differences were found to be significant ($p > 0.16$).

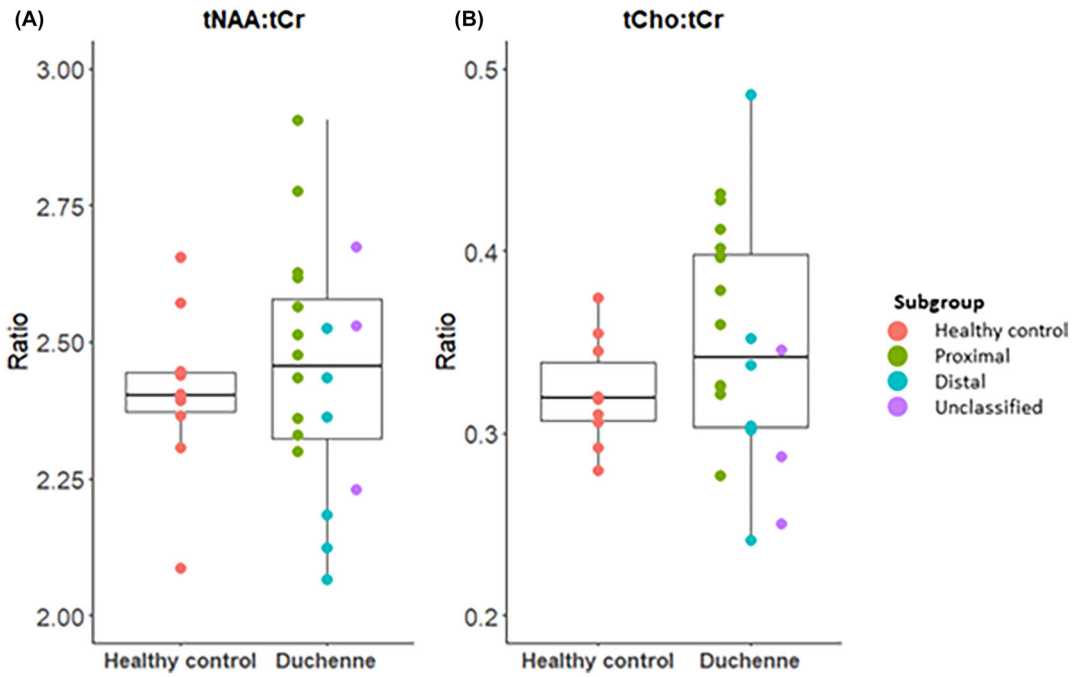

FIGURE 5 Scatterplots for the metabolite ratios of tNAA:tCr (A) and tCho:tCr (B). None of the between-group differences were found to be significant ($p > 0.05$). For the Duchenne subgroup, a proximal mutation affects the Dp427 form only (i.e., assumed to be linked to neurons), and distal corresponds to a mutation affecting both Dp427 and Dp140 forms (i.e., assumed to be linked to neurons and glial cells).

10991492, 0, Downloaded from https://analyticalsciencejournals.onlinelibrary.wiley.com/doi/10.1002/nbm.5212 by Newcastle University, Wiley Online Library on [24/07/2024]. See the Terms and Conditions (https://onlinelibrary.wiley.com/terms-and-conditions) on Wiley Online Library for rules of use; OA articles are governed by the applicable Creative Commons License

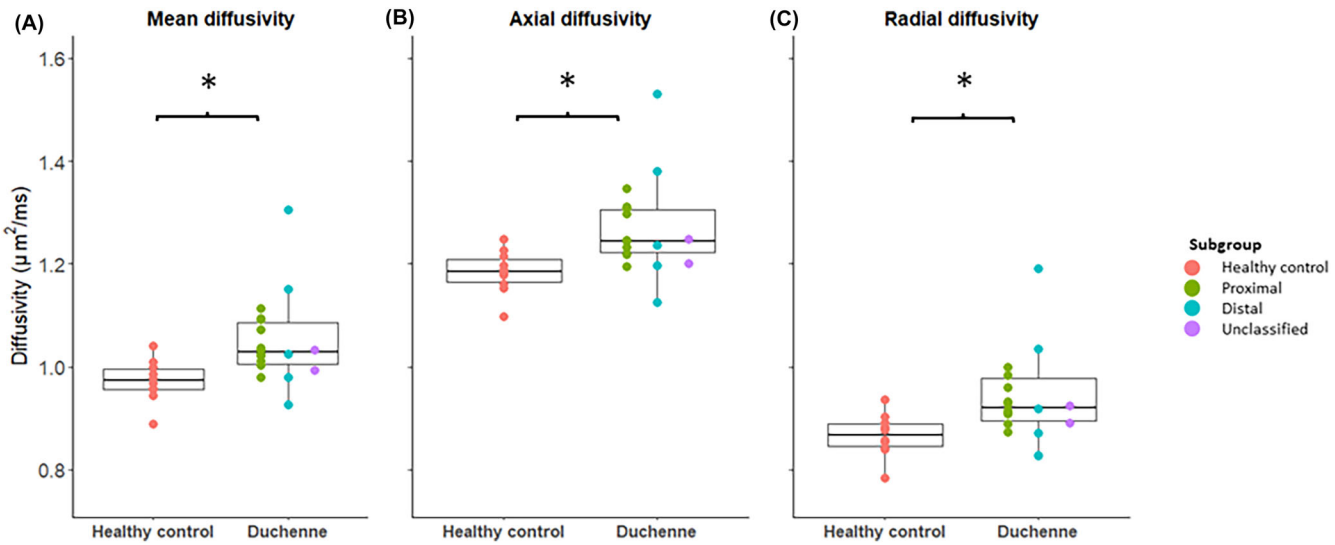

FIGURE 6 Scatterplots for the between-group differences of water diffusion for MD (A), AD (B), and RD (C). *All between-group differences were found to be significant ($p < 0.05$). For the Duchenne subgroup, a proximal mutation affects the Dp427 form only (i.e., assumed to be linked to neurons), and distal corresponds to a mutation affecting both Dp427 and Dp140 forms (i.e., assumed to be linked to neurons and glial cells).

3.3 | Water diffusion properties

MD within the VOI was higher for patients with DMD compared with HCs ($p = 0.0001$, Figure 6). Post hoc analysis to assess if the higher MD was a result of axial or radial diffusion showed both increased RD ($p = 0.011$) and increased AD ($p = 0.012$). FA did not show any differences between DMD and HCs ($p = 0.212$; Table 2).

4 | DISCUSSION

In this study, we aimed to determine if microstructural changes in water diffusion properties in the white matter in the DMD brain are driven by intra- or extracellular factors. We previously showed, using DTI alone, that white matter microstructure is altered in DMD.[23] However, due to the ubiquitous nature of water molecules, we could not conclude if our measurement reflected changes in the intra- or extracellular space microstructure. In this context, we used combined DTI and DWS acquisitions to detect cell-specific changes in vivo in patients with DMD. We hypothesized that metabolite ADC would be altered together with water ADC. We found no significant difference in metabolite ADC while reproducing a significant increase in water MD/RD/AD coefficient in the same VOI. No differences in metabolite levels were found as the ratios did not differ between groups, which is consistent with previous MRS results within this region.[28,29]

DWS measurements were performed at a diffusion time of about 64 ms, resulting in a typical diffusion distance for metabolites of about 5–10 μm. As suggested by previous studies,[41,42] our metabolite DWS measurement is mainly sensitive to the diffusion in long fibres (i.e., astrocytic processes, neuronal dendrites, etc.). Consequently, we hypothesize that our DWS measurement framework cannot inform us of changes at the level of the cell bodies. Based on the observation that metabolite ADC did not change between DMD patients and controls, we hypothesize that there are no cytomorphological changes at the intracellular level within the astrocytic processes and neuronal dendrites in DMD patients. This suggests that these effects are therefore not contributing to changes in white matter diffusion. In general, DWS studies have a lower sensitivity compared with DTI due to low metabolite concentration compared with water, and as a result studies are performed in a relatively large VOI and with long acquisition times. Here, we acquired data in a relatively short acquisition time (3 min 44 s compared with a minimum of 15 min) at 3 T, but due to stringent quality control we could obtain DWS data in HCs with similar values and variability compared with our previous findings.[29,43,44]

The potential sensitivity of DWS to pathology has been shown in studies focussing for instance on multiple sclerosis, including the same number of patients and HCs as our study. These studies showed that patients with multiple sclerosis had a reduced NAA diffusivity.[41,42] In DMD patients, the variation in the ADC of tCho (0.037 μm^2/ms) seems to differ more compared with the variation in the ADCs of tNAA and tCr (both 0.023 μm^2/ms). This larger variation could be attributable to the underlying cytomorphological changes due to the different dystrophin isoforms, which might have a different effect on glial cells compared with neurons. However, due to our relatively small group sizes, we were unable to differentiate between the different mutation types in patients with DMD.

10991492, 0, Downloaded from https://analyticalsciencejournals.onlinelibrary.wiley.com/doi/10.1002/nbm.5212 by Newcastle University, Wiley Online Library on [24/07/2024]. See the Terms and Conditions (https://onlinelibrary.wiley.com/terms-and-conditions) on Wiley Online Library for rules of use; OA articles are governed by the applicable Creative Commons License

As expected, no differences in FA between DMD and controls were observed. As in our previous results, the FA map showed only differences in the occipital lobe.[23] The differences we found in diffusion properties of water (MD, RD, and AD)[23] could be due to multiple factors, such as reduced fibre density, increased membrane permeability, and/or decreased structural organization or demyelination.[45] Dp140 and/or Dp71 isoforms are associated with astrocytes.[17,18] A study on DMD astrocytes showed an altered morphology, altered proliferative activity, and decreased AQP4 expression.[21] This points to a potentially altered permeability of the membrane influencing the altered diffusion properties of water, with extracellular and possibly astrocytic changes possibly related to AQP4,[21] contributing to the increase in apparent water diffusivity.

Another possible explanation for our results is the use of glucocorticoid treatment in patients with DMD. A previous study on glucocorticoid use in systemic and inhaled glucocorticoid users showed an altered white matter integrity.[46] In addition, work with Cushing patients showed that glucocorticoids have an impact on white matter and that oligodendrocytes are very sensitive to glucocorticoids.[47–49] Disentangling the contribution of glucocorticoids to DTI from the absence of dystrophin as the main pathophysiology is only possible if patients not taking glucocorticoids are included. This is an ethical dilemma, as glucocorticoids significantly slow down the disease progression and are part of the standard of care.

In conclusion, by combining DWS and DTI, we aimed to distinguish between intra- and extracellular diffusion in white matter. We found preserved diffusion of the cell-specific metabolites tNAA, tCho, and tCr in our parietal white matter VOI. Our DWS results indicate preserved cell fibre microstructure. Consequently, water changes could be dominated by altered white matter microstructure at the extracellular level. The reported decrease in AQP4 expression in DMD[21] also points to potential astrocytic permeability changes, although no intracellular glial changes were detected with DWS. This illustrates the benefits of combined DTI and DWS to gain a better understanding of the underlying mechanisms in a clinical setting.

ACKNOWLEDGEMENTS

The authors would like to acknowledge all patients and their caregivers for participating.

Several authors of this publication are members of the Netherlands Neuromuscular Center (NL-NMD) and the European Reference Network for rare neuromuscular diseases ERN-EURO-NMD.

CONFLICT OF INTEREST STATEMENT

The LUMC receives support from Philips Healthcare and trial support from ImagingDMD-UF outside the submitted work.

ORCID

Rosanne Govaarts https://orcid.org/0000-0002-4550-3977
Nathalie Doorenweerd https://orcid.org/0000-0003-2932-4327
Chloé F. Najac https://orcid.org/0000-0002-7804-2281
Emma M. Broek https://orcid.org/0000-0001-5713-0533
Kieren G. Hollingsworth https://orcid.org/0000-0002-3135-8131
Erik H. Niks https://orcid.org/0000-0001-5892-5143
Itamar Ronen https://orcid.org/0000-0002-6872-4895
Hermien E. Kan https://orcid.org/0000-0002-5772-7177

REFERENCES

1. Banihani R, Smile S, Yoon G, et al. Cognitive and neurobehavioral profile in boys with Duchenne muscular dystrophy. *J Child Neurol*. 2015;30(11):1472-1482. doi:10.1177/0883073815570154
2. Conway KC, Mathews KD, Paramsothy P, et al. Neurobehavioral concerns among males with dystrophinopathy using population-based surveillance data from the Muscular Dystrophy Surveillance, Tracking, and Research Network. *J Dev Behav Pediatr*. 2015;36(6):455-463. doi:10.1097/DBP.0000000000000177
3. Darmahkasih AJ, Rybalsky I, Tian C, et al. Neurodevelopmental, behavioral, and emotional symptoms common in Duchenne muscular dystrophy. *Muscle Nerve*. 2020;61(4):466-474. doi:10.1002/mus.26803
4. Hendriksen JGM, Vles JSH. Neuropsychiatric disorders in males with Duchenne muscular dystrophy: frequency rate of attention-deficit hyperactivity disorder (ADHD), autism spectrum disorder, and obsessive–compulsive disorder. *J Child Neurol*. 2008;23(5):477-481. doi:10.1177/0883073807309775
5. Hendriksen RGF, Vles JSH, Aalbers MW, Chin RFM, Hendriksen JGM. Brain-related comorbidities in boys and men with Duchenne muscular dystrophy: a descriptive study. *Eur J Paediatr Neurol*. 2018;22(3):488-497. doi:10.1016/J.EJPN.2017.12.004
6. Lee AJ, Buckingham ET, Kauer AJ, Mathews KD. Descriptive phenotype of obsessive compulsive symptoms in males with Duchenne muscular dystrophy. *J Child Neurol*. 2018;33(9):572-579. doi:10.1177/0883073818774439
7. Pangalila RF, Van Den Bos GA, Bartels B, Bergen M, Stam HJ, Roebroeck ME. Prevalence of fatigue, pain, and affective disorders in adults with Duchenne muscular dystrophy and their associations with quality of life. *Arch Phys Med Rehabil*. 2015;96(7):1242-1247. doi:10.1016/J.APMR.2015.02.012
8. Ricotti V, Mandy WPL, Scoto M, et al. Neurodevelopmental, emotional, and behavioural problems in Duchenne muscular dystrophy in relation to underlying dystrophin gene mutations. *Dev Med Child Neurol*. 2016;58(1):77-84. doi:10.1111/DMCN.12922

10991492, 0, Downloaded from https://analyticalsciencejournals.onlinelibrary.wiley.com/doi/10.1002/nbm.5212 by Newcastle University, Wiley Online Library on [24/07/2024]. See the Terms and Conditions (https://onlinelibrary.wiley.com/terms-and-conditions) on Wiley Online Library for rules of use; OA articles are governed by the applicable Creative Commons License

9. Holder E, Maeda M, Bies RD. Expression and regulation of the dystrophin Purkinje promoter in human skeletal muscle, heart, and brain. *Hum Genet*. 1996;97(2):232-239. doi:10.1007/BF02265272
10. Muntoni F, Torelli S, Ferlini A. Dystrophin and mutations: one gene, several proteins, multiple phenotypes. *Lancet Neurol*. 2003;2(12):731-740. doi:10.1016/S1474-4422(03)00585-4
11. Lidov HGW, Selig S, Kunkel LM. Dp140: a novel 140 kDa CNS transcript from the dystrophin locus. *Hum Mol Genet*. 1995;4(3):329-335. doi:10.1093/HMG/4.3.329
12. Austin RC, Morris GE, Howard PL, Klamut HJ, Ray PN. Expression and synthesis of alternatively spliced variants of Dp71 in adult human brain. *Neuromuscul Disord*. 2000;10(3):187-193. doi:10.1016/S0960-8966(99)00105-4
13. Austin RC, Howard PL, D'Souza VN, Klamut HJ, Ray PN. Cloning and characterization of alternatively spliced isoforms of Dp71. *Hum Mol Genet*. 1995;4(9):1475-1483. doi:10.1093/hmg/4.9.1475
14. Fort PE, Sene A, Pannicke T, et al. Kir4.1 and AQP4 associate with Dp71-and utrophin-DAPs complexes in specific and defined microdomains of Muller retinal glial cell membrane. *Glia*. 2008;56(6):597-610. doi:10.1002/glia.20633
15. Lederfein D, Levy Z, Augier N, et al. A 71-kilodalton protein is a major product of the Duchenne muscular dystrophy gene in brain and other non-muscle tissues. *Proc Natl Acad Sci USA*. 1992;89(12):5346-5350. doi:10.1073/PNAS.89.12.5346
16. Tadayoni R, Rendon A, Soria-Jasso LE, Cisneros B. Dystrophin Dp71: the smallest but multifunctional product of the Duchenne muscular dystrophy gene. *Mol Neurobiol*. 2012;45(1):43-60. doi:10.1007/s12035-011-8218-9
17. Culligan K, Ohlendieck K. Diversity of the brain dystrophin–glycoprotein complex. *J Biomed Biotechnol*. 2002;2(1):31-36. doi:10.1155/S1110724302000347
18. Waite A, Brown SC, Blake DJ. The dystrophin–glycoprotein complex in brain development and disease. *Trends Neurosci*. 2012;35(8):487-496. doi:10.1016/j.tins.2012.04.004
19. Doorenweerd N, Mahfouz A, van Putten M, et al. Timing and localization of human dystrophin isoform expression provide insights into the cognitive phenotype of Duchenne muscular dystrophy. *Sci Rep*. 2017;7(1):12575. doi:10.1038/s41598-017-12981-5
20. Naidoo M, Anthony K. Dystrophin Dp71 and the neuropathophysiology of Duchenne muscular dystrophy. *Mol Neurobiol*. 2020;57(3):1748-1767. doi:10.1007/S12035-019-01845-W
21. Lange J, Gillham O, Alkharji R, et al. Dystrophin deficiency affects human astrocyte properties and response to damage. *Glia*. 2022;70(3):466-490. doi:10.1002/GLIA.24116
22. Doorenweerd N, Dumas EM, Ghariq E, et al. Decreased cerebral perfusion in Duchenne muscular dystrophy patients. *Neuromuscul Disord*. 2017;27(1):29-37. doi:10.1016/j.nmd.2016.10.005
23. Doorenweerd N, Straathof CS, Dumas EM, et al. Reduced cerebral gray matter and altered white matter in boys with Duchenne muscular dystrophy. *Ann Neurol*. 2014;76(3):403-411. doi:10.1002/ANA.24222
24. Tracey I, Thompson CH, Dunn JF, et al. Brain abnormalities in Duchenne muscular dystrophy: phosphorus-31 magnetic resonance spectroscopy and neuropsychological study. *Lancet*. 1995;345(8960):1260-1264. doi:10.1016/S0140-6736(95)90923-0
25. Ronen I, Valette J. Diffusion-weighted magnetic resonance spectroscopy. *eMagRes*. 2015;4:733-750. doi:10.1002/9780470034590.emrstm1471
26. Ronen I, Ercan E, Webb A. Axonal and glial microstructural information in white matter obtained with diffusion weighted magnetic resonance spectroscopy at 7T. *Front Integr Neurosci*. 2013;7:13. doi:10.3389/FNINT.2013.00013
27. Palombo M, Shemesh N, Ronen I, Valette J. Insights into brain microstructure from in vivo DW-MRS. *NeuroImage*. 2018;182:97-116. doi:10.1016/j.neuroimage.2017.11.028
28. Rae C, Scott RB, Thompson CH, et al. Brain biochemistry in Duchenne muscular dystrophy: a ^{1}H magnetic resonance and neuropsychological study. *J Neurol Sci*. 1998;160(2):148-157. doi:10.1016/S0022-510X(98)00190-7
29. Doorenweerd N, Hooijmans M, Schubert SA, et al. Proton magnetic resonance spectroscopy indicates preserved cerebral biochemical composition in Duchenne muscular dystrophy patients. *J Neuromuscul Dis*. 2017;4(1):53-58. doi:10.3233/JND-160201
30. Fu Y, Dong Y, Zhang C, et al. Diffusion tensor imaging study in Duchenne muscular dystrophy. *Ann Transl Med*. 2016;4(6):109. doi:10.21037/atm.2016.03.19
31. Preethish-Kumar V, Shah A, Kumar M, et al. In vivo evaluation of white matter abnormalities in children with Duchenne muscular dystrophy using DTI. *Am J Neuroradiol*. 2020;41(7):1271-1278. doi:10.3174/ajnr.A6604
32. Brooke MH, Fenichel GM, Griggs RC, et al. Clinical Investigation of Duchenne muscular dystrophy. Interesting results in a trial of prednisone. *Arch Neurol*. 1987;44(8):812-817. doi:10.1001/archneur.1987.00520200016010
33. Duan D, Goemans N, Takeda S, Mercuri E, Aartsma-Rus A. Duchenne muscular dystrophy. *Nat Rev Dis Primers*. 2021;7(1):13. doi:10.1038/s41572-021-00248-3
34. Smith SM. Fast robust automated brain extraction. *Hum Brain Mapp*. 2002;17(3):143-155. doi:10.1002/HBM.10062
35. Zhang Y, Brady M, Smith S. Segmentation of brain MR images through a hidden Markov random field model and the expectation-maximization algorithm. *IEEE Trans Med Imaging*. 2001;20(1):45-57. doi:10.1109/42.906424
36. Jenkinson M, Beckmann CF, Behrens TEJ, Woolrich MW, Smith SM. FSL. *NeuroImage*. 2012;62(2):782-790. doi:10.1016/J.NEUROIMAGE.2011.09.015
37. Provencher SW. Estimation of metabolite concentrations from localized in vivo proton NMR spectra. *Magn Reson Med*. 1993;30(6):672-679. doi:10.1002/mrm.1910300604
38. Govindaraju V, Young K, Maudsley AA. Proton NMR chemical shifts and coupling constants for brain metabolites. *NMR Biomed*. 2000;13(3):129-153. doi:10.1002/1099-1492(200005)13:33.0.CO;2-V
39. Near J, Harris AD, Juchem C, et al. Preprocessing, analysis and quantification in single-voxel magnetic resonance spectroscopy: experts' consensus recommendations. *NMR Biomed*. 2021;34(5):e4257. doi:10.1002/nbm.4257
40. Leemans A, Jeurissen B, Sijbers J, Jones DK. ExploreDTI: a graphical toolbox for processing, analyzing, and visualizing diffusion MR data. *Proc Int Soc Magn Reson Med*. 2009;17:3537.
41. Wood ET, Ercan E, Sati P, Cortese ICM, Ronen I, Reich DS. Longitudinal MR spectroscopy of neurodegeneration in multiple sclerosis with diffusion of the intra-axonal constituent N-acetylaspartate. *NeuroImage Clin*. 2017;15:780-788. doi:10.1016/j.nicl.2017.06.028

10991492, 0, Downloaded from https://analyticalsciencejournals.onlinelibrary.wiley.com/doi/10.1002/nbm.5212 by Newcastle University, Wiley Online Library on [24/07/2024]. See the Terms and Conditions (https://onlinelibrary.wiley.com/terms-and-conditions) on Wiley Online Library for rules of use; OA articles are governed by the applicable Creative Commons License

42. Wood ET, Ronen I, Techawiboonwong A, et al. Investigating axonal damage in multiple sclerosis by diffusion tensor spectroscopy. *J Neurosci*. 2012; 32(19):6665-6669. doi:10.1523/JNEUROSCI.0044-12.2012
43. Kan HE, Techawiboonwong A, van Osch MJP, et al. Differences in apparent diffusion coefficients of brain metabolites between grey and white matter in the human brain measured at 7 T. *Magn Reson Med*. 2012;67(5):1203-1209. doi:10.1002/mrm.23129
44. Ellegood J, Hanstock CC, Beaulieu C. Trace apparent diffusion coefficients of metabolites in human brain using diffusion weighted magnetic resonance spectroscopy. *Magn Reson Med*. 2005;53(5):1025-1032. doi:10.1002/mrm.20427
45. Assaf Y, Pasternak O. Diffusion tensor imaging (DTI)-based white matter mapping in brain research: a review. *J Mol Neurosci*. 2008;34(1):51-61. doi:10.1007/s12031-007-0029-0
46. van der Meulen M, Amaya JM, Dekkers OM, Meijer OC. Association between use of systemic and inhaled glucocorticoids and changes in brain volume and white matter microstructure: a cross-sectional study using data from the UK Biobank. *BMJ Open*. 2022;12(8):e062446. doi:10.1136/bmjopen-2022-062446
47. van der Werff SJA, Andela CD, Nienke Pannekoek J, et al. Widespread reductions of white matter integrity in patients with long-term remission of Cushing's disease. *NeuroImage Clin*. 2014;4:659-667. doi:10.1016/j.nicl.2014.01.017
48. Pires P, Santos A, Vives-Gilabert Y, et al. White matter involvement on DTI-MRI in Cushing's syndrome relates to mood disturbances and processing speed: a case–control study. *Pituitary*. 2017;20(3):340-348. doi:10.1007/s11102-017-0793-y
49. Pires P, Santos A, Vives-Gilabert Y, et al. White matter alterations in the brains of patients with active, remitted, and cured Cushing syndrome: a DTI study. *Am J Neuroradiol*. 2015;36(6):1043-1048. doi:10.3174/ajnr.A4322

SUPPORTING INFORMATION

Additional supporting information can be found online in the Supporting Information section at the end of this article.

How to cite this article: Govaarts R, Doorenweerd N, Najac CF, et al. Probing diffusion of water and metabolites to assess white matter microstructure in Duchenne muscular dystrophy. *NMR in Biomedicine*. 2024;e5212. doi:10.1002/nbm.5212

10991492, 0, Downloaded from https://analyticalsciencejournals.onlinelibrary.wiley.com/doi/10.1002/nbm.5212 by Newcastle University, Wiley Online Library on [24/07/2024]. See the Terms and Conditions (https://onlinelibrary.wiley.com/terms-and-conditions) on Wiley Online Library for rules of use; OA articles are governed by the applicable Creative Commons License